MOX–Report No. 10/2011

Multiscale computational analysis of degradable polymers

Zunino, P.; Vesentini, S.; Porpora, A.; Soares, J.S.; Gautieri, A.; Redaelli, A.

MOX, Dipartimento di Matematica "F. Brioschi"
Politecnico di Milano, Via Bonardi 9 - 20133 Milano (Italy)

mox@mate.polimi.it http://mox.polimi.it

Multiscale computational analysis of degradable polymers *

P. Zunino♯, S. Vesentini, A. Porpora♯, J.S. Soares, A. Gautieri, A. Redaelli

February 17, 2011

♯ MOX– Modellistica e Calcolo Scientifico
Dipartimento di Matematica "F. Brioschi"
Politecnico di Milano
P.zza Leonardo da Vinci 32, 20133 Milano, Italy
paolo.zunino@polimi.it

Abstract

Degradable materials have found a wide variety of applications in the biomedical field ranging from sutures, pins and screws for orthopedic surgery, local drug delivery, tissue engineering scaffolds, and endovascular stents. Polymer degradation is the irreversible chain scission process that breaks polymer chains down to oligomers and, finally, to monomers. These changes, which take place at the molecular scale, propagate through the space/time scales and not only affect the capacity of the polymer to release drugs, bu also hamper the overall mechanical behavior of the device, whose spatial scale is denoted as macro-scale. A bottom-up multiscale analysis is applied to model the degradation mechanism which takes place in PLA matrices. The macroscale model is based on diffusion-reaction equations for hydrolytic polymer degradation and erosion while the microscale model is based on atomistic simulations to predict the water diffusion as a function of the swelling degree of the PLA matrix. The diffusion coefficients are then passed to the macroscale model. In conclusion, the proposed multiscale analysis is capable to predict the evolution with time of several properties of water/PLA mixtures, according to the change of relevant indicators such as the extent of degradation and erosion of the PLA matrix.

1 Introduction

Biodegradable materials offer tremendous potential for the development of implantable devices and systems for treating disease. Currently, biodegradable polymers are used

*This work has been supported by the Italian Institute of Technology with the Grant Models and methods for degradable materials and the European Research Council Advanced Grant Mathcard, Mathematical Modelling and Simulation of the Cardiovascular System, Project ERC 2008 AdG 227058

in diverse applications ranging from absorbable sutures [24], orthopedic implants [37], drug delivery devices [23], scaffolds for tissue engineered constructs [1], medicated and biodegradable stents [42]. When applications involve either negligible or well-known design requirements, the design of these classes of implants are greatly facilitated. However, in situation where the requirements are more complex, either in implants featuring complex geometries or in implants under conditions that influence the course of degradation and erosion, the design process is usually inhibited by the lack of rational models of biodegradable material behavior [42, 32]. In order to advance from prototype status to a reliable human-implant devices, device designers must therefore rely on a combination of intuition and trial-and-error approaches that often fail due to two major reasons: (i) the lack of models able to describe the evolution of the material as it degrades and erodes, and (ii) the difficulty to collect reliable experimental data quantifying and characterizing this behavior. Theoretical models to predict polymer degradation and erosion would seem to be important tools for a number of different applications. If drug elution is to be part of the therapy, drug delivery profiles should be programmable at the design stage. For load bearing implants, mechanical properties and structural integrity of the implant as well as their evolution should be accounted for. Because the implant is ultimately absorbed, structural breakdown and loss of function must be predicted and carefully designed for.

Polymer degradation is the deleterious change in properties of the material due to irreversible changes in its chemical structure. A biodegradable polymer is a polymer in which the degradation is mediated at least partially by a biological system [35]. More precisely, polymer degradation is the chain scission process that breaks polymer chains down to oligomers and finally to monomers, ultimately resulting in a decrease of molecular weight. Polymers degrade by several different mechanisms, depending on their inherent chemical structure and on the environment conditions to which they are subjected. The prevailing mechanism of biological degradation for synthetic biodegradable aliphatic polyesters (the most commonly employed biodegradable polymers in the medical such as polyglycolic acid and polylactic acid [16]) is scission of the hydrolytically unstable backbone chain by passive hydrolysis. By tailoring the polymer backbone with hydrolysable functional groups, the polymer chains become labile to an aqueous environment and their ester linkages are cleaved by absorbed water. There are two key factors that influence: (i) co-polymer composition and (ii) water uptake. Water adsorption, the first step of degradation is dependent on polymer hydrophilicity.

The diffusion of water into the polymer bulk and the chain scission reaction compete against each other in the process of polymer erosion. Erosion is caused by degradation and is the process of dissolution or wearing away of degradation byproducts, resulting in mass loss from the polymer bulk. Erosion is by far much more complex than degradation inasmuch as the number of parameters that potentially might influence the process is considerably larger. Two main modes of erosion can be systematized from widely established empirical evidence [7]. If degradation is fast, the diffusing water is absorbed quickly by hydrolysis and is hindered from penetrating deep into the polymer bulk. In this case, degradation and consequently erosion are restricted to the surface of the polymer, a phenomenon referred to as heterogeneous or surface erosion [45].

This type of erosion changes if degradation is slower than the rate of diffusion of water through the polymer. In this case, water cannot be absorbed quickly enough to be hindered from reaching deep into the polymer and the reaction takes place through its entire swollen bulk, a behavior which has been termed homogeneous or bulk erosion [45]. Nevertheless, surface or bulk erosion modes are two extremes and the erosion of a polymer usually shows characteristics of both.

Hydrolysis is a very intricate process that occurs at the molecular level, as a variety of different scission pathways can occur simultaneously and concurrently [48]. Although the reactivity of each bond might be equal when considered individually, the large number of repeating units and their inherent steric environment, weak links, and branches may influence locally the rate of reaction. Ultimately, experiments with gel permeation chromatography provide data to model the mechanism of degradation [33, 34], and kinetic parameters are obtained from the evolution of experimentally obtained molecular weight distributions. An approach pioneered by Kuhn [22] and Montroll and Simha [31] employs combinatorial statistic to derive analytical solutions of the evolution of molecular weight distribution assuming that bond scission can be described with a known probability density function (e.g. equiprobable random scission, central Gaussian, or parabolic) and only for some limited simple initial conditions. Unfortunately, the applicability of such elegant exact solutions to real systems is limited essentially due to simplifying assumptions necessary for the analytical treatment of the problem. A second technique to model polymer degradation relies on the system of differential equations which describe the depolymerization rates of individual bonds that upon integration yield the time evolution of the molecular weight distribution [4]. However, the complete kinetic scheme that includes all the individual rate constents for each reacting bond could represent an enormous number of coupled differential equations even for modest size macromolecules. A third common method employs Monte Carlo simulations applied to populations of polymer chains [21, 9, 6], a versatile approach that can technically overcome the simplifying assumptions needed on the others, but realistic simulations may require an excessive amount of computational resources, results are usually subjected to large statistical errors, and may be in fact unnecessary when compared with simpler approaches.

Erosion is a much more complex phenomenon to model, not only because of the interplay between different physical mechanisms as well as due to the dramatic changes that occur in the polymer as it erodes. The choice of effective modeling tools is, however, not straightforward, and two main approaches can be currently identified: models based on differential equations that consider the erodible material as a continuum and stochastic models that describe degradation and erosion as a probabilistic event (cf. [40] for comprehensive review). In the scope of the deterministic approach, Heller and Baker [17] pioneered with a simple model for degradation from bulk eroding polymers consisting of steady state water diffusion coupled with a reaction equation describing the kinetics of the degradation mechanism. Lee [25] proposed a simplified model for surface erosion and drug release from polymer films based on the movements of two fronts, a diffusion front and an erosion front. Thombre, Joshi, and Himmelstein [47, 20, 46] proposed a comprehensive theory for drug release, water penetration, and erosion and

corroborated the theoretical findings with experimental results. Similar methods based on diffusion equations that account degradation and erosion in more complex systems have been developed since [5, 26, 36]. On the other hand, stochastic models complemented with Monte Carlo simulations to simulate surface or bulk eroding polymers have been developed (cf. Zygourakis [50] and Gopferich and co-workers [13, 12, 14]). Erosion is described as being a probabilistic event and the polymer bulk as a grid of pixels. By removing eroded pixels from the grid, the stochastic evolution of a polymeric matrix was obtained and experimentally measurable parameters, such as porosity and weight loss, were calculated. Erosion fronts and a distinction between erosion modes were inferred from the results and their fit to experimental data allowed the determination of erosion rate constents. Although such models have shown good performance because of their versatility to account a multitude of phenomena occurring due to degradation and erosion (e.g. the formation of voids inside the polymer bulk as well as in the treatment of moving erosion fronts), their associated computational cost is generally much larger than with the solution of partial differential equations. Nonetheless, the common difficulties associated with erosion modeling are still present: (i) the necessity of choosing a priori the mode of erosion to model for, (ii) the difficulty arising from modeling preferential degradation of the amorphous phase, and (iii), the most difficult aspect, the incorporation of changes in the microstructure caused by erosion , which are usually specified within phenomenological reasoning. While the first two aspects have been tackled to some extent, the latter is still an open problem that will need a huge amount of insightful theoretical modeling and careful experimental characterization.

The authors have introduced a general class of mixture models to study water uptake, degradation, erosion, and drug release from degradable polydisperse polymeric matrices [43]. The model is comprehensive starting from individual polymer scission reaction all the way up to the macro-scale diffusion, allows for the systematic characterization of the mass loss during the erosion process, and unifies both bulk and surface extremes of the erosion mode spectrum. The mixture is characterized by a finite number of constituents describing the polydisperse polymeric system, i.e. each representing collection of chains whose size belongs to a finite interval of degree of polymerization. In order to account for water uptake and drug release, two additional constituents (water and drug) constitute the mixture. Our approach is based on basic and widely established physical laws: (i) constituents diffuse individually accordingly to Fick's law of diffusion, (ii) hydrolysis is accounted as chemical reactions that result in the production/destruction of polymeric chains and water consumption, and (iii) balances of mass of constituents yield coupled partial differential equations that govern the reaction-diffusion system. Constitutive relationships characterizing the diffusivity of each constituent and the scission reaction rates must be specified; once known, the problem is closed and can be solved given initial and boundary conditions. Previously, we have proposed several broad assumptions in the derivation of phenomenologically reasoned constitutive relationships; nonetheless, their sufficient generality resulted in a general class of mathematical models that describe the polymer degradation and erosion. Our approach truly unified the behaviors of surface and bulk erosion and the nondimensionalization of the governing equations allowed the identification of the Thiele modulus,

the ratio between characteristic timescales of diffusion and reaction, which is a key parameter in conferring the shift between bulk or surface erosion behavior to the solution of the equations.

Our model would have immediate direct impact in the design of biodegradable implants if these phenomenologically derived general constitutive behaviors were better characterized in regard to particular polymeric systems of interest. One possible strategy would be to perform an unprecedented series of experiments with the goal of characterizing the diffusivity of each constituent (water, drug, monomers, oligomers, etc) in a changing media (as the network degrades and erodes). To overcome this unfeasible plan, we have developed a coupling between the macroscale of the biodegradable polymer bulk, which is governed by the reaction diffusion system, and the microscale of chemical reactions and molecular diffusion, which with the aid of atomistic simulations characterizes locally the diffusion of constituents in the polymer bulk accordingly to its changing microstructure. Atomistic or molecular dynamics simulations cannot yet provide further insight into the rates of reactions taking place, but on the other hand, have been able to characterize the diffusion coefficient of molecules in a polymeric network with quite success (cf. [18] and references therein). With these new tools, we are able to provide unique information into the macroscale model in the specification of the local diffusivities of mixture constituents. More precisely, the macroscale model provides local molecular configurations (i.e. set of polymer chains and water) as input for the microscale model, which then outputs the local diffusivities of the constituents at the macroscale level. Unfortunately, molecular dynamics simulations are extremely expensive computationally, and hence this dynamic coupling strategy would not result in a practical solution. To this end, we developed lumping strategies to parametrize the range of local molecular configurations and statically couple both scales.

2 A mixture model for water uptake, degradation and erosion from polymeric matrices

Following the lines of [43], we develop a general tridimensional model for the degradation of PLA upon water absorption and subsequent hydrolysis. First, we describe the nature of the model and its governing equations and then complement it with specific initial and boundary conditions. The main difficulty consists in the definition of suitable constitutive laws for the model coefficients. The novelty of the present work consists in the application of atomistic simulation to estimate the most significant properties of PLA along degradation, giving rise to a multiscale description of the material.

2.1 Macroscale governing equations for a polymer mixture

We describe a polydisperse polymeric network as a collection of different linear chains of repeating units. Each chain is characterized by its degree of polymerization, x, defined as the number of repeating units. The system is discretized into N number of constituents by defining N mutually exclusive equidistent partitions $P_i = [\bar{x}_i - \bar{x}_1/2, \bar{x}_i +$

$\bar{x}_1/2[$, for $i = 1,\ldots,N$, of length $\bar{x}_1$ of the degree of polymerization spectrum. Each partition P_i represents the class of chains whose average degree of polymerization is $\bar{x}_i$.

Diffusion driven by negative density gradients is the driving force for mass transport. To account for diffusion, we introduce a spatial coordinate $\mathbf{x}$ characterizing the location of a particle of the mixture with volume $\mathrm{d}V$. At each particle, water, drug, and N polymeric constituents coexist. Since the mascroscale spans over the entire length of the polymer matrix, external boundaries have to be taken into account. In this respect, an open system is considered as water penetrates into the polymer matrix from the outside aqueous environment and polymeric mass is lost to the exterior. The mass balances for each individual constituent yield the system of reaction-diffusion equations constituting the mathematical model.

Let $\rho_i = \rho_i(\mathbf{x},t)$ be the partial density of chains of average degree of polymerization $\bar{x}_i$ in a representative control volume, dV, that corresponds to point $\mathbf{x}$ at time t and let $w_i = \rho_i/\sum_i \rho_i$ be the weight fraction of chains of length $\bar{x}_i$. Let $\rho_w(\mathbf{x},t)$ be the partial density of water. We also denote with $\tilde{\rho} = \sum_i \rho_i$ the partial density of all polymer sub-fractions and with $\rho = \rho_w + \sum_i \rho_i$ the total density of the mixture. Finally, for the forthcoming description, we denote with $\Upsilon = (\rho_w, \rho_1, \ldots, \rho_N)$ the vector of partial densities of each component that completely identifies the state of the mixture, i.e. this is the *state space* of the macroscale model. For notation cleanliness, we shall omit the dependence on space and time ($\mathbf{x}$ and t) of partial densities.

Mass can be neither created nor destroyed, but in the present case, polymer chains and water can diffuse in/out of $\mathrm{d}V$ through its boundary. Moreover, polymeric constituents interconvert from one to another due to scission reactions. The mass balance of each constituent in $\mathrm{d}V$ states that the time rate of change of mass existing in $\mathrm{d}V$ is equal to the divergence of the diffusive flux plus time rates of production and/or destruction in chemical reactions. As $\mathrm{d}V \to 0$, mass balances of each polymeric constituent yield the system of N reaction-diffusion equations

$$\partial_t \rho_i = \nabla \cdot (D_i \nabla \rho_i) + \sum_{j=1}^{N} A_{ij} \rho_j, \text{ for } i = 1,\ldots,N \tag{1}$$

where D_i is the diffusivity of chains of average degree of polymerization $\bar{x}_i$ and coefficients A_{ij} are the reaction coefficients corresponding to chain cleavage due to hydrolysis. More precisely, a chain of average degree of polymerization $\bar{x}_i$ can be cleaved at $j = 1,\ldots,i-1$ different scission locations (each composed of $\bar{x}_1$ individual polymeric bonds) to yield chains of smaller average degree of polymerization, $\bar{x}_j$ and $\bar{x}_{i-j}$. All $i-1$ possible outcomes of scission of a chain of degree of polymerization $\bar{x}_i$ are

$$\bar{x}_i \xrightarrow{k_{i,j}} \bar{x}_j + \bar{x}_{i-j}, \text{ for } i = 1,\ldots,N,\ j = 1,\ldots,i-1$$

The depolymerization kinetics of populations of individual molecules can be described by means of a system of ordinary differential equations (cf. [33, 34]). Let $n_i = n_i(t)$ denote the number of chains of average degree of polymerization $\bar{x}_i$ existing at time t. As $\mathrm{d}V \to 0$, the relationship between partial density ρ_i and number of molecules n_i is

$\rho_i(\mathbf{x},t) = n_i(\mathbf{x},t)\bar{x}_i M_0/\mathrm{d}V$, where M_0 is the molecular mass of one monomeric unit and $\bar{x}_i M_0$ is the molecular weight of polymer subfractions of length $\bar{x}_i$. In a closed system, the rate of change of n_i is given by,

$$\dot{n}_i = -\sum_{j=1}^{i-1} k_{i,j} n_i + \sum_{j=i+1}^{N} (k_{j,i} + k_{j,j-i}) n_j, \text{ for } i = 1,\ldots,N.$$

Then, equation (1) is complemented by the following expressions:

$$A_{ij} = \begin{cases} 0 & \text{if } j < i \\ -\sum_{m=1}^{i-1} k_{i,m} & \text{if } j = i \\ (k_{j,i} + k_{j,j-i}) \frac{\bar{x}_i}{\bar{x}_j} & \text{if } j > i \end{cases}$$

The combination of equation (1) and (2) results in a multiscale description of polymer degradation and erosion, as it combines a molecular description of chain scission at the molecular level (second term on the right hand side of (1)) with macroscopic Fick's law of diffusion (first term of the right hand side of (1)).

Water diffuses in the polymeric matrix and hydrolysis is accounted as a sink of water, i.e.

$$\partial_t \rho_w = \nabla \cdot (D_w \nabla \rho_w) - f_w \tag{2}$$

where $\rho_w = \rho_w(\mathbf{x},t)$ and D_w are the partial density and the diffusivity of water. Reaction term $f_w > 0$ accounts for water consumption: one water molecule is consumed with each scission reaction, i.e.

$$\bar{x}_1 \cdot \begin{bmatrix} \text{bond of scission} \\ \text{location } j \text{ of chain } \bar{x}_i \end{bmatrix} + \mathrm{H_2O} \xrightarrow{k_{i,j}} \text{scission event}$$

The rate $k_{i,j}$ is the rate of reaction of scission location j composed of $\bar{x}_1$ bonds, hence the rate of water consumption in the scission event is $k_{i,j}/\bar{x}_1$. The rate of change of the number of water molecules $n_w = n_w(\mathbf{x},t)$ in a representative volume $\mathrm{d}V$ is given by

$$\dot{n}_w = -\sum_{i=1}^{N} \sum_{j=1}^{i-1} \frac{k_{i,j}}{\bar{x}_1} n_i$$

which, with the relationship between n_w and ρ_w as $\mathrm{d}V \to 0$, $\rho_w = n_w M_w/\mathrm{d}V$ (where M_w is the molecular mass of water), yields the water consumption due to the chemical reaction in Eq.(6)

$$f_w = \sum_{i=1}^{N} \sum_{j=1}^{i-1} k_{i,j} \frac{M_w}{M_0 \bar{x}_1} \frac{\rho_i}{\bar{x}_i}$$

2.2 Initial and boundary value problem

Boundary and initial conditions depend on the application that one has in mind. In our case, we aim to model the coating of a medicated stent, which is a thin polymer

layer covering the surface of a cardiovascular stent. For this reason, the geometry of the polymer matrix can be thought of as a thin slab. Then, the governing equations can be reduced to one spatial dimension, z, the coordinate across the thickness ($z \in [0, L]$ where L is the coating thickness). The polymer network starts out dry, i.e. $\rho_w(z,0) = 0$ and the initial state of the polydisperse polymeric system is homogeneous, i.e. independent of z, and is characterized by an initial degree of polymerization distribution $w^0 = w^0(x)$ and an initial total (dry) polymer density ρ^0 . The initial weight fraction of chains of average degree of polymerization $\bar{x}_i, w_i$ are obtained with Eq. (1) and the initial conditions of the polymeric constituents densities are set as $\rho_i(z,0) = w_i^0 \rho^0$ for $i = 1, \ldots, N$. In what follows, indexes 0 and ∞ will refer to the state of the mixture at $t \to 0$ and $t \to \infty$, respectively.

At $z = 0$ we apply impermeable boundary conditions

$$\partial_z \rho_w|_{z=0} = 0, \ \partial_z \rho_i|_{z=0} = 0$$

with the meaning that any constituent is not able to leave from the polymeric matrix and penetrate the stainless steel bulk of the stent. At $z = L$, the polymer contacts surrounding water or biological tissue. Water permeates through the interface according to the following law,

$$-D_w \partial_z \rho_w|_{z=L} = \pi_w(\rho_w|_{z=L} - A)$$

where π_w is the permeability of the interface to water molecules and A is a partition coefficient (with $A \in [0,1]$), which accounts that water uptake increases as the polymer erodes, leading to an eventual total replacement of the swollen network with a mixture solely composed of pure water.

Proceeding similarly, boundary conditions for polymeric constituents are

$$-D_i \partial_z \rho_i|_{z=L} = \pi_i \rho_i|_{z=L}$$

The permeability π_i of the polymer matrix to different polymer sub-fractions at the interface with aqueous outside will be defined later on in order to make sure that the boundary conditions for polymeric constituents shift from an approximation of a perfect sink condition for the smaller chains towards a no-flux condition for the larger molecules. More precisely, smaller chains are readily dissolved in the surrounding water or absorbed by the tissue when they reach the boundary, i.e. $\rho_1(L,t) \simeq 0, \ t > 0$, whereas the longer chains are unable to diffuse due to their size and entanglements in the polymeric matrix; hence $\partial_z \rho_N(L,t) \simeq 0, \ t > 0$. In between, a shift occurs gradually with both terms of $-D\partial_z \rho_i = \pi_i \rho_i$ having the same relevance for species of medium degree of polymerization.

2.3 Constitutive laws

Constitutive relationships for the diffusivity of each constituent and for the reaction rates must be specified. The mechanisms of diffusion and reaction are the only physical mechanisms that need constitutive specification and once known, the model is closed and can be solved.

Diffusion depends on the nature of the constituent in question and on the local characteristics of the mixture on which is diffusing. In the most general case this is taken into account by the following expressions

$$D_w = D_w(\rho_w, \rho_1, \ldots, \rho_N), \quad D_i = D_i(\rho_w, \rho_1, \ldots, \rho_N)$$

In the forthcoming sections, we will apply atomistic simulations of molecular diffusion into a polymer mixture in order to provide a simplified characterization of such models.

To describe the permeability of the mixture at the interface with the external medium, we assume that permeability and diffusivity are proportional. Then, the permeability π_w, π_i are given by

$$\frac{\pi_w}{\pi_w^0} = \frac{D_w}{D_w^0}, \quad \frac{\pi_i}{\pi_i^0} = \frac{D_i}{D_i^0}$$

where π_w^0 and and D_w^0 represent the permeability and the diffusivity of water in a non-degraded mixture, which will be provided by atomistic simulations. To determine the reference permeability π_i^0 we apply again the proportionality between permeability and diffusivity,

$$\frac{\pi_i^0}{\pi_w^0} = \frac{D_i^0}{D_w^0}$$

that combined with the previous expression gives,

$$\pi_i = D_i \frac{\pi_w^0}{D_w^0}$$

The saturation of non degraded mixture with respect to water is modeled by condition is determined by $A^0 < 1$ (that will be later determined according to data taken by [18]). As erosion of the polymer at the interface leads to a decrease in the total polymer density, denoted with $\tilde{\rho} = \sum_i \rho_i$, we propose the linear relationship

$$A = 1 - (1 - A^0) \frac{\tilde{\rho}|_{z=L}}{\rho_w^\infty}$$

such that $A \to 1$ when $\tilde{\rho}|_{z=L} \to 0$, which at saturation equilibrium results in a mixture characterized by $\rho_w \to \rho_w^\infty$ and $\rho_i \to 0$ for all $i = 1, \ldots, N$, i.e. the network was replaced by pure surrounding fluid.

We finally take into account hydrolysis. One common tool to describe the localization of the scission event along large chains is a scission probability density function, which distinguishes the likelihood of scission among scission locations in a chain of average degree of polymerization $\bar{x}_i$, i.e. the relationships among $k_{i,j}$ with i fixed and $j \in 1, 2, \ldots, i-1$. Some frequently encountered scission probability density functions are: random, parabolic, and central scission (cf. [20, 21] for details). Aliphatic polyesters degrade by passive hydrolysis and are usually characterized by random scission events. Random scission is defined with a constent probability density function

along the length of the chain, i.e. $k_{i,1} = k_{i,2} = \cdots = k_{i,i-1}$, for all $i = 2, \ldots, N$. Considering k as the rate of hydrolysis of the particular type of polymeric bond, all $k_{i,j}$ are given by

$$k_{i,j} = k\bar{x}_1, \text{ for } i = 2, \ldots, N \text{ and } j = 1, \ldots, i-1$$

Hydrolysis happens due to the presence of water, hence its rate depends on the partial density ρ_w. Because water might not be homogeneously distributed over the network, the rate of reaction depends implicitly on space and leads to inhomogeneous degradation. Following similar studies (cf. [40]), random hydrolysis is a 1st order reaction with water, i.e. the polymeric bond has reaction rate that follows a linear relationship with partial density of water such that

$$k = k(\rho_w) = \bar{k}\rho_w$$

where $\bar{k}$ is a constent reaction rate. In such way, bilinear terms (each featuring ρ_w and one ρ_i) appear in the reaction terms of Eqs. (1) and (2). Autocatalysis, i.e. when the rate of scission depends on the presence of residual monomer, is not accounted with this constitutive specification.

3 Molecular diffusion into polymeric networks

We aim to apply a protocol based on atomistic simulations to predict the water and polymer diffusion as a function of the composition of the water/polymer mixture, characterized by the coordinates in the state space $\Upsilon = (\rho_w, \rho_1, \ldots, \rho_N)$ previously introduced. The diffusion coefficients are then passed to the macroscale model.

3.1 Generation and equilibration of the atomistic models of PLA

To generate atomistic models of PLA we have applied Materials Studio 4.4 (Accelrys, Inc.) and the COMPASS force field [44]. The repeating unit of PLA is available as standard model in Materials Studio. The polymeric chains with the desired length are generated starting from the repeating units using the Build Polymers tool of Materials Studio. Finally, we generate solvated amorphous bulk models containing PLA and water using the Amorphous Cell tool of Materials Studio. The polymeric chains are solvated in a periodic box with a total atom number varying from 6,000 atoms (for quasi-dry systems) to 35,000 atoms (for highly solvated systems), as depicted in Figure 1

The initial geometries of the bulk models are refined following the procedure which consists in a series of MD calculations at different temperature and ensembles in order to obtain chain redistribution within the periodic cell [18, 10, 19, 11]. Specifically, we perform a preliminary minimization followed by a sequence of nine MD simulations (see Table 1). MD molecular dynamics simulations are carried using the Discover module and the COMPASS force field implemented in Materials Studio. Nonbonding interactions are computed using a cutoff for neighbor list at 1 nm, with a switching function between 0.85 and 0.95 nm for Van der Waals and Coulomb interactions.

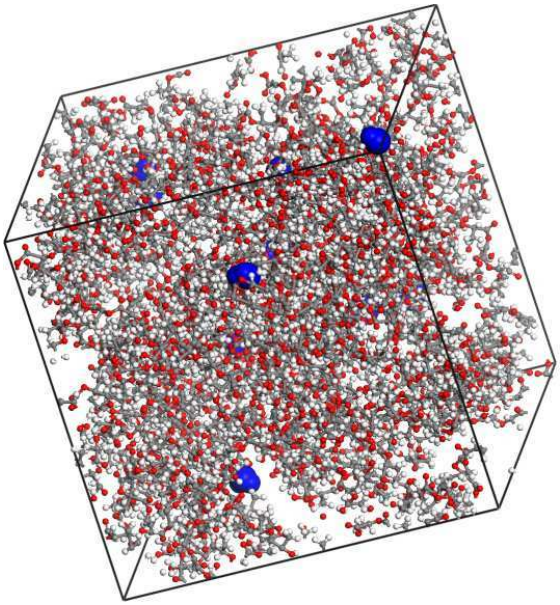

Figure 1: Atomistic bulk model of quasi-dry PLA matrix (water molecules in blue color).

We carefully checked that the potential energy, temperature, pressure and density reached a stable value after each step of the equilibration procedure. The latest (#9) simulation has been employed to validate the models by comparing the average density during the NPT dynamics with the experimental one.

Finally, in order to obtain water and polymer diffusivity by means of an atomistic model of the polymer mixture, we select an ensemble of M (water or polymer) molecules in the model and we compute their mean square displacement $MSD(t)$. Denoting with

$$\langle \mathbf{r}(t)^2 \rangle = \frac{1}{M} \sum_{m=1}^{M} \mathbf{r}_m(t)^2$$

the averaging over all the particles, the mean square displacement is defined as

$$MSD(t) = \langle |\mathbf{r}(t) - \mathbf{r}(0)|^2 \rangle$$

The diffusion coefficient D of water/polymer molecule is then calculated using Einstein's relation

$$D = \lim_{t \to \infty} MSD(t)/(6t)$$

Manipulating Einstein's formula one easily obtain that for sufficiently large times $\log(6D) + \log(t) = \log\big(MSD(t)\big)$. Then, the realm of normal diffusion (also known as Fickian diffusion) is reached when $\log\big(MSD(t)\big)$ is a linear function of time with unit slope. The validity of this fundamental property is equivalent to say that the application of Fick's law to derive equation (1) and (2) is correct.

Table 1: Summary of the simulation protocol applied to obtain equilibrated bulk model of PLA matrices.

Simulation	Ensemble	Time	Time step	Temperature	Pressure
#1	NVT	0.2 ps	0.1 fs	300 K	-
#2	NVT	2 ps	1 fs	600 K	-
#3	NVT	100 ps	1 fs	300 K	-
#4	NPT	60 ps	1 fs	300 K	0 GPa
#5	NVT	20 ps	1 fs	750 K	-
#6	NVT	20 ps	1 fs	600 K	-
#7	NVT	20 ps	1 fs	450 K	-
#8	NVT	100 ps	1 fs	300 K	-
#9	NPT	100 ps	1 fs	300 K	0 GPa

4 Multiscale analysis

We formulate here different strategies for the interaction of the micro and the macroscale models. We start from the algorithms that most tightly couple the two models and we progressively simplify them, in order to balance the accuracy of the methodology with a reasonable computational cost.

4.1 Input/Output description of the models

According to the previous derivation, the macroscale model for polymer mixtures is not computable, because it needs to determine water and polymer diffisivities in the mixture to close governing equations and boundary conditions. More precisely, the input/output structure of the macroscale model can be described as follows:

Input: given $D_w(\rho_w,\rho_1,\dots,\rho_N)$ and $D_i(\rho_w,\rho_1,\dots,\rho_N)$

Compute: for any (z,t) solve the following problem

$$\begin{cases} \partial_t\rho_w = \nabla\cdot\big(D_w\nabla\rho_w\big) - \bar{k}\frac{M_w}{M_0\bar{x}_1}\sum_{i=1}^{N}\frac{i-1}{i}\rho_w\rho_i, \\ \partial_t\rho_i = \nabla\big(D_i\nabla\rho_i\big) - (i-1)\bar{k}\bar{x}_1\rho_w\rho_i + 2\bar{k}\bar{x}_1\rho_w\sum_{j=i+1}^{N}\frac{i}{j}\rho_j, \\ \partial_z\rho_w|_{z=0} = 0, \quad -D_w\partial_z\rho_w|_{z=L} = \pi_w(\rho_w|_{z=L} - A) \\ \partial_z\rho_i|_{z=0} = 0, \quad -D_i\partial_z\rho_i|_{z=L} = \pi_i\rho_i|_{z=L} \\ \rho_w(z,0) = 0, \quad \rho_i(z,0) = w_i^0\tilde{\rho}^0 \end{cases} \tag{3}$$

Output: determine the mixture partial densities: $\rho_w(t,z),\rho_1(t,z),\dots,\rho_N(t,z)$ that can be further post-processed to compute other indicators that characterize the mixture composition.

Reminding that $\Upsilon = (\rho_w,\rho_1,\dots,\rho_N)$ denotes the state variables of the model, the *macroscale* model can be described by means of the following input-output scheme:

$$D_w(\Upsilon), D_i(\Upsilon) \overset{\text{macro}}{\Longrightarrow} \Upsilon(t,z)$$

Concerning the microscale model, we observe that, since the dimension of the state space $\Upsilon(t,z) = (\rho_w(t,z), \rho_1(t,z), \ldots, \rho_N(t,z))$ is considerably large, namely $N+1$, it would be a challenging task to design an ensemble of atomistic simulations sufficient to characterize constitutive laws of type $D_w = D_w(\rho_w, \rho_1, \ldots, \rho_N)$, $D_i = D_i(\rho_w, \rho_1, \ldots, \rho_N)$. By consequence, we first introduce a *lumped state space*, identified by a vector valued function $\mathscr{F} : \mathbb{R}^{N+1} \to \mathbb{R}^M$ with $M \leq N+1$, such that it is possible to initialize an atomistic PLA model on the basis of $\mathscr{F}(\Upsilon)$ solely. This assumption will remarkably simplify the interacton between the micro and the macro scale models. According to the results reported in the forthcoming sections, we select a the follwing lumped state space with $M = 2$:

1. the degree of swelling,

$$\mathscr{F}_1(\Upsilon(t,z)) = \phi_w(\Upsilon(t,z)) = \frac{\rho_w(t,z)}{\rho_w(t,z) + \sum_{i=1}^{N} \rho_i(t,z)}$$

   which describes the ratio of water in the entire mixture.

2. the (weight) average degree of polymerization,

$$\mathscr{F}_2(\Upsilon(t,z)) = \bar{x}(\Upsilon(t,z)) = \sum_{i=1}^{N} w_i(t,z) \cdot \bar{x}_i$$

   which describes the average size of polymeric chains in the mixture and always satisfies $\bar{x}_1 \leq \mathscr{F}_2 \leq \bar{x}_N$.

We notice that this simplification involves some loss of information. On one hand, according to degradation of polymeric chains, a polymer mixture is generally *polydisperse*, i.e. it is composed by a collection of several sub-fractions. On the other hand, the selected lumped state space is not able to represent polydispersity and it replaces a given distribution of sub-fractions with *monodisperse* mixture of equivalent average degree of polymerization. Mathematically speaking, this corresponds to say that function $\mathscr{F}$ is surjective, for any $M < N+1$. In this framework, we sketch below the input/output description of the microscale model:

Input: given $(\phi_w, \bar{x})$ generate the corresponding atomistic model of PLA.

Compute: select some tracers molecules (either water or polymer) to evaluate molecular diffusion. Then, perform MD simulations to compute their trajectories $r(t)$ over a sufficiently large time span. Finally perform the mean square displacement analysis combined with Einstein's relation in order to estimate the molecular diffusivity $D_w(\phi_w, \bar{x})$, $D_i(\phi_w, \bar{x})$ of the water or polymer tracers in a given PLA mixture.

Output: the model provides the molecular diffusivity of water and polymer molecules, i.e. independent values $D_w(\phi_w, \bar{x})$, $D_i(\phi_w, \bar{x})$, into a given PLA/water mixture.

A synthetic input/output relation for the microscale model reads as follows:

$$\mathscr{F}(\Upsilon) \overset{\text{micro}}{\Longrightarrow} D_w(\mathscr{F}(\Upsilon)), D_i(\mathscr{F}(\Upsilon))$$

that will be complemented with the application of the macroscale model in the lumped state space,

$$D_w(\mathscr{F}(\Upsilon)), D_i(\mathscr{F}(\Upsilon)) \overset{\text{macro}}{\Longrightarrow} \Upsilon \Longrightarrow \mathscr{F}(\Upsilon)$$

We finally notice that the set up of the microscale model is pointwise or local, that is it applies to any single point (t,z) of the macroscale domain.

4.2 Multiscale coupling strategies

First, we address a *fully coupled* algorithm, that best exploits the interaction among micro and macro-sacles. Let t^n the time levels corresponding to time discretization of the macroscale model, and let $z_j \in [0,L]$ the nodes associated to space discretization. For any (t^n, z_j), the algorithm consists in the following iterative steps for $k = 1, \ldots$:

1. Set a guess for the state of the system i.e. $\Upsilon^{(0)}(t^n, z_j)$.
2. Solve the microscale model:

$$\mathscr{F}(\Upsilon^{(k-1)}(t^n, z_j)) \overset{\text{micro}}{\Longrightarrow} D_w^{(k)}(t^n, z_j), D_i^{(k)}(t^n, z_j)$$

3. Solve the macroscale model:

$$D^{(k)}(t^n, z_j),\ D_i^{(k)}(t^n, z_j) \overset{\text{macro}}{\Longrightarrow} \Upsilon^{(k)}(t^n, z_j)$$

   Then, compute $\mathscr{F}(\Upsilon^{(k)}(t^n, z_j))$.

Reminding that the computational cost of a single solution of the microscale model is considerable, because of the complexity of a polymeric network, this algorithm is not yet affordable with standard computational devices. Furthermore, we notice that the cost of this algorithm exponentially increases with the number of space dimensions accounted by the macroscale model. Indeed, realistic applications in three space dimensions would be practically unachievable. For this reason, we consider the following simplification, which can be classified as a *time staggered and space averaged* coupled algorithm. As it will be discussed later on, such simplification is acceptable for bulk eroding polymers, where spatial gradients of densities are almost negligible, i.e. $\nabla_{\mathbf{x}} \Upsilon(t, \mathbf{x}) \simeq 0$ for any $t > 0$ and for any $\mathbf{x} \in \Omega$. Let us define the following spatial average for $\mathscr{F}$:

$$\overline{\mathscr{F}}(\Upsilon(t,z)) = \int_0^L \mathscr{F}(\Upsilon(t,z))dz$$

Then, given the initial state of the system i.e. $\Upsilon(t^0, z)$, for any $n > 0$ we perform the following steps:

1. Solve the microscale model at time t^{n-1}:

$$\overline{\mathscr{F}}(\Upsilon(t^{n-1},z)) \overset{\text{micro}}{\Longrightarrow} \overline{D}_w(t^{n-1}),\overline{D}_i(t^{n-1})$$

2. Advance in time and solve the macroscale model at time t^n:

$$\overline{D}_w(t^{n-1}),\overline{D}_i(t^{n-1}) \overset{\text{macro}}{\Longrightarrow} \Upsilon(t^n,z_j)$$

   Then, compute $\overline{\mathscr{F}}(\Upsilon(t^n,z))$.

We notice that this algorithm considerably reduces the number of calls to the microscale model and makes it independent on the number of space dimensions of the macroscale equations.

In alternative to the previous algorithms, which turn out to be computationally expensive in any case, we propose the following *static coupling strategy* to feed the macroscale model with data provided by microscale sumulations. For the sake of simplicity, we only refer to a generic diffusivity $D(\Upsilon)$ that stands for either $D_w(\Upsilon)$ or $D_i(\Upsilon)$. Let $\{\Upsilon_p\}_{p=1}^P$ be different mixture configurations and let $\mathbf{D} = \{D(\overline{\mathscr{F}}(\Upsilon_p))\}_{p=1}^P$ be the vector defined as follows,

$$\overline{\mathscr{F}}(\Upsilon_p) \overset{\text{micro}}{\Longrightarrow} D(\overline{\mathscr{F}}(\Upsilon_p))$$

We aim to determine a function $\mathscr{D}(\overline{\mathscr{F}}(\Upsilon))$ that suitably approximate its discrete analog $\mathbf{D} \in \mathbb{R}^P$. First, a parametrization for $\mathscr{D}$ with polynomials is obtained by defining as $\mathbf{q} \in \mathbb{N}^{M=2}$ a multi-index with $q = \sum_{k=1,2} \mathbf{q}$ and

$$\mathscr{D}(\overline{\mathscr{F}}) = \mathscr{D}^{\mathbf{a}}\big(\sum_{q=0}^{Q} a_{\mathbf{q}} \overline{\mathscr{F}}_1^{q_1} \overline{\mathscr{F}}_2^{q_2}\big)$$

where $\mathbf{a}$ is the vector of coefficients $\{a_{\mathbf{q}}\}_{q=1}^Q$. For the well posedness of the forthcoming algorithm we have to make sure that $P \geq Q$. Then we introduce a vector function $\mathbf{D}^{\mathbf{a}} : \mathbb{R}^Q \to \mathbb{R}^P$ defined as $\mathbf{D}^{\mathbf{a}} = \{D^{\mathbf{a}}(\overline{\mathscr{F}}(\Upsilon_p))\}_{p=1}^P$ such that,

$$D^{\mathbf{a}}(\overline{\mathscr{F}}(\Upsilon_p)) = \mathscr{D}^{\mathbf{a}}\big(\sum_{q=0}^{Q} a_{\mathbf{q}} \overline{\mathscr{F}}_1^{q_1}(\Upsilon_p) \overline{\mathscr{F}}_2^{q_2}(\Upsilon_p)\big)$$

Then, the optimal parameters $\mathbf{a}$ such that $\mathscr{D}^{\mathbf{a}}$ best fits the data $\mathbf{D}$ are determined as follows,

$$\mathbf{a}^* = \text{argmin}_{\mathbf{a}} \|\mathbf{D} - \mathbf{D}^{\mathbf{a}}\|_2$$

In such way we determine an explicit representation of functions $\mathscr{D}_w(\Upsilon)$ and $\mathscr{D}_i(\Upsilon)$ representing a closure of the macroscale model (3) that is now completely solvable.

Table 2: Density of the water/polymer mixture in g/cm^3 for different average degree of polymerization, $\bar{x}$, (colums) and % of water content, ϕ_w, (rows).

		ϕ_w					
		0%	20%	40%	60%	80%	100%
$\bar{x}_i$	600	1.1703	1.1424	1.0836	1.0566	1.0177	0.9871
	300	1.1763	1.1415	1.0984	1.0623	1.0161	0.9871
	150	1.1634	1.1419	1.0976	1.0582	1.0168	0.9871
	75	1.1677	1.1482	1.1033	1.0536	1.0170	0.9871
	30	1.1815	1.1422	1.0953	1.0570	1.0175	0.9871
	1	1.0497	1.0196	1.0071	0.9953	0.9866	0.9871

5 Computational analysis of polymer degradation

5.1 Computational results of the microscale model

The diffusion of water in PLA matrices is modeled considering monodisperse systems with different level of PLA degradation and swelling (i.e., water content). We generated 30 different molecular models of PLA matrices, characterized by different degree of polymerization (monodisperse systems with 600, 300, 150, 75, 30 and 1 monomers per chain, respectively) (see Fig. 2) and different degree of swelling (with 2%, 20%, 40%, 60% and 80% of water). Additionally, we studied a system containing pure water for validating reasons.

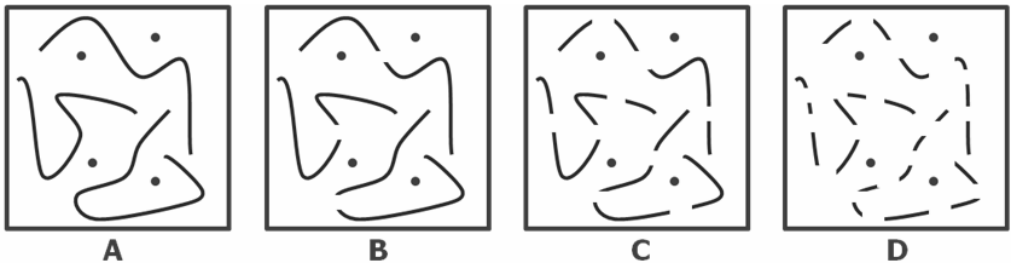

Figure 2: Sketch of the quasi-dry PLA matrices (2% water) studied in this work, from non degraded matrix (A) to partially degraded (B and C) and highly degraded (D).

As a preliminary validation of the atomistic models we analyze the density of the quasi-dry PLA matrices, see Table 2, showing that the predicted density ($\simeq 1.18 g/cm^3$) is close to experimental density of PLA ($1.24 g/cm^3$). On the other hand, the final density of the pure water systems ($0.98 g/cm^3$) well matches the water density. For the systems with intermediate water content the density decrease linearly from the density of quasi-dry PLA to the density of pure water.

We then proceed with the calculation of the water diffusivity in PLA matrices by

Table 3: Diffusion coefficient of water ($10^{-6} cm^2/s$) with respect to monomers per chain (colums) and % of water content (rows).

		ϕ_w					
		2%	20%	40%	60%	80%	100%
$\bar{x}_i$	600	0.41	3.39	13.5	24.2	36.8	42.0
	300	0.42	4.97	13.2	24.5	33.9	42.0
	150	0.40	4.56	13.8	22.2	35.6	42.0
	75	0.47	2.79	12.0	23.9	34.7	42.0
	30	0.39	3.56	12.3	24.2	35.8	42.0
	1	0.51	4.38	16.4	25.9	36.8	42.0

means of in silico experiments run for a simulated time of 7 ns. As a validation of the approach we calculated the self diffusion coefficient of water, obtaining a value of $42.0 \cdot 10^{-6} cm^2/s$, close to the experimental value ($22.7 \cdot 10^{-6} cm^2/s$). The analysis of the water diffusivity values in PLA (see Table 3) shows that the diffusivity coefficient spans two orders of magnitude (from 10^{-7} to $10^{-5} cm^2/s$) and is mainly affected by the water content. Indeed, the diffusion coefficient increases almost linearly with the degree of swelling, while it is little or no affected by the degree of polymerization. It is important to observe that the Einstein relation holds only if the regime of normal diffusion is reached. Reminding that normal diffusion is reached when $\log(MSD(t))$ is an affine linear function with respect to $\log(t)$ with unit slope, we observe that the normal diffusion of water is reliably reached during the data production runs of 7 ns, since the aforementioned slope ranges from 0.87 to 1.00. Consequently, the diffusivity coefficients obtained for water transport in the polymer matrix can be assumed to be reliable.

As similar procedure may be applied to calculate $D_i(\phi_w, \bar{x})$, resorting to a Table similar to 3 for any $i = 1, \ldots, N$. Although all aforementioned simplifications, this task requires a large number of microscale simulations. To fulfill this task with a moderate computational cost, we have initially performed the simpler investigation of calculating the matrix of values $D_i(\phi_w, \bar{x}_i)$. This corresponds to estimate the diffusivity of a polymer chain of length $\bar{x}_i$ into a mixture of the same average degree of polymerization.

The results (see Table 4) show that the polymer diffuses much less than water due to its larger molecular weight. The exceptions are the systems with single PLA monomers (highly degraded matrices) for which a much higher PLA diffusion constant is obtained. This is likely due to the low molecular weight of PLA monomers. The analysis of the results for PLA diffusivity shows that the polymer diffusion coefficient depends on the swelling, while it is not affected by the polymer degradation, showing a behavior similar to water transport. This consideration allows us to assume that the diffusivity of polymer sub-fractions of length $\bar{x}_i$ into a mixture of average degree of polymerization $\bar{x} \neq \bar{x}_i$ may be very similar to the sub-fraction of length $\bar{x}_i$ in itself. In practice, we conclude that $D_i(\phi_w, \bar{x}_i) \simeq D_i(\phi_w, \bar{x})$ for any $\bar{x}_1 \leq \bar{x} \leq \bar{x}_N$. This is equivalent to say that

Table 4: Diffusion coefficient ($10^{-8} cm^2/s$) of PLA chains of length $\bar{x}_i$ into themselves (columns) with respect to % of water content (rows).

		ϕ_w					
		2%	20%	40%	60%	80%	100%
$\bar{x}_i$	600	0.33	1.3	3.5	3.7	42.5	-
	300	0.50	1.5	5.2	4.8	35.2	-
	150	0.45	0.8	8.4	6.8	38.6	-
	75	0.37	1.2	5.0	6.8	24.0	-
	30	0.51	1.6	3.8	6.8	27.6	-
	1	480	530	540	590	650	-

Table 4 represents the diffusivity of polymer subfraction $\bar{x}_i$ in all possible water/polymer mixtures.

Finally, we must note that normal diffusion is not reached for the polymer diffusivity, since the slope of $\log(MSD(t))$ presents values below 1 (with the exception of PLA monomers, for which the normal diffusion is instead reached). This shows that nanoseconds time scales are insufficient to reach the normal diffusion regime for large molecules. Consequently, the PLA diffusivity coefficients can only be assumed as trend indicators or top range values, since coefficients calculated out of the normal diffusion regime provide higher values.

5.2 Results and validation for the macroscale model

As proposed in [43] to perform numerical simulations it is convenient to rewrite problem (3) in non dimensional form. First, the longest PLA chains that we consider feature $\bar{x}_N = 600$ monomers,the shortest $\bar{x}_1 = 15$ units and the entire spectrum is subdivided into $N = 40$ classes. To this purpose, we select the polymer thickness $L = 10\mu\, m$ as the characteristic length, $\tau = \bar{k}\rho_w^\infty\, s$ as the characteristic time, $D_w^0 = 4.1 \times 10^{-7}\, cm^2/s$ as reference diffusivity and finally $\rho_w^\infty = 0.98,\ \rho^0 = 1.18\ g/cm^3$ as the density of pure water and non degraded PLA respectively. Then, without change of notation, the non-dimensional form of equations (3) reads as follows,

$$\begin{cases} \partial_t \rho_w = \Lambda \nabla \cdot \left(\mathscr{D} \nabla \rho_w\right) - K \sum_{i=1}^{N} \frac{i-1}{i} \rho_w \rho_i, \\ \partial_t \rho_i = \Lambda \nabla \left(\mathscr{D}_i \nabla \rho_i\right) - (i-1)\bar{x}_1 \rho_w \rho_i + 2\bar{x}_1 \rho_w \sum_{j=i+1}^{N} \frac{i}{j} \rho_j, \\ \partial_z \rho_w|_{z=0} = 0, \quad -\mathscr{D}_w \partial_z \rho_w|_{z=L} = \Gamma \pi_w (\rho_w|_{z=L} - A) \\ \partial_z \rho_i|_{z=0} = 0, \quad -\mathscr{D}_i \partial_z \rho_i|_{z=L} = \Gamma \pi_i \rho_i|_{z=L} \\ \rho_w(z,0) = 0, \quad \rho_i(z,0) = w_i^0 \tilde{\rho}^0 \end{cases} \tag{4}$$

where the diffusivity of water and polymer are determined by atomistic simulations, as previously described, while the non-dimensional numbers

$$\Lambda = \frac{D_w^0}{L^2 \bar{k} \rho_w^\infty},\ K = \frac{M_w \rho^0}{M_0 \bar{x}_1 \rho_w^\infty},\ \Gamma = \frac{L \pi_w^0}{D_w^0}, \tag{5}$$

We estimate the Thiele number as $\Lambda = 7 \times 10^4$, where $\bar{k} = 5 \times 10^{-2}\ day^{-1}$ is taken from [43] and references therein, which confirms that PLA is a bulk eroding polymer, $\Gamma = 10^{-3}$ with the assumption $\pi_w^0 / D_w^0 = 1$, $K = 0.0042$ with $\bar{x}_1 = 15$, $M_0 = 90$, $M_w = 18\, g/mol$ are the molecular weights of PLA and water respectively. Finally, the saturation of water into dry polymer is estimated by [41] as $1\, g\ water/g\ PLA$, i.e. $A^0 = 0.5\%$.

For the estimation of the diffusivity of water and polymer with respect to the degree of swelling ϕ_w and the average degree of polymerization $\bar{x}$, we have applied the static multiscale coupling strategy previously described. In particular, for water we obtain,

$$\begin{aligned}\mathscr{D}_w(\phi_w, \bar{x}) = &-3.524 + 92.974\phi_w + 0.0137\bar{x} - 0.115\phi_w\bar{x} + 17.540\phi_w^2 \\ &- 0.0000213\bar{x}^2 + 0.0916\phi_w^2\bar{x} + 0.000183\phi_w\bar{x}^2 - 0.000142\phi_w^2\bar{x}^2\end{aligned}$$

For the diffusivity D_i we have considered a slightly different approach. Denoting with $\mathbf{D}_i$ the data-set relative to Table 3 and with $\mathbf{D}_i^{\mathbf{a}}$ the parametrized function to be estimated, we have solved the following least square problem,

$$\mathbf{a}^* = \arg\min_{\mathbf{a}} \| \log(\mathbf{D}_i^{\mathbf{a}} - \mathbf{D}_i) \|$$

As a result of that we obtain,

$$\begin{aligned}\mathscr{D}_i(\phi_w, \bar{x}) = \exp(&-4.531 + 5.483\phi_w + 0.000642\bar{x} - 0.00074\phi_w\bar{x} - 0.693\phi_w^2 \\ &- 0.00000115\bar{x}^2 + 0.002\phi_w^2\bar{x} - 0.000004\phi_w\bar{x}^2 + 0.000005\phi_w^2\bar{x}^2)\end{aligned}$$

that ensures that $\mathscr{D}_i(\phi_w, \bar{x})$ is always positive. A visual comparison of the interpolants $\mathscr{D}_w(\phi_w, \bar{x}), \mathscr{D}_i(\phi_w, \bar{x})$ with the corresponding control points, that are entries of Tables 3 and 4 respectively, is reported in Figure 3.

The solution of problem (4) is provided by numerical approximation schemes. In particular, we have exploited Lagrangian finite elements for the space discretization, by resorting to a semi-discrete problem that has been fully discretized with backward finite difference schemes to advance in time. For further details, we refer to [39, 15]. The main difficulty in the approximation of the problem at hand consists in the efficient solution of the nonlinear system of equations arising from the fully discrete scheme. To this aim, we have applied the damped Newton method proposed in [8].

The results of numerical simulations for

$$\rho_w(t,z),\ \tilde{\rho}(t,z) = \sum_i \rho_i(t,z),\ \rho_{31}^{40} = \sum_{i=31}^{40} \rho_i(t,z),\ \rho_1^{10} = \sum_{i=1}^{10} \rho_i(t,z)$$

are reported in Figure 4. Depending on the value of the Thiele modulus, Λ, different modes of degradation and erosion occurred. For PLA $\Lambda = 17000$ diffusion occurs at a

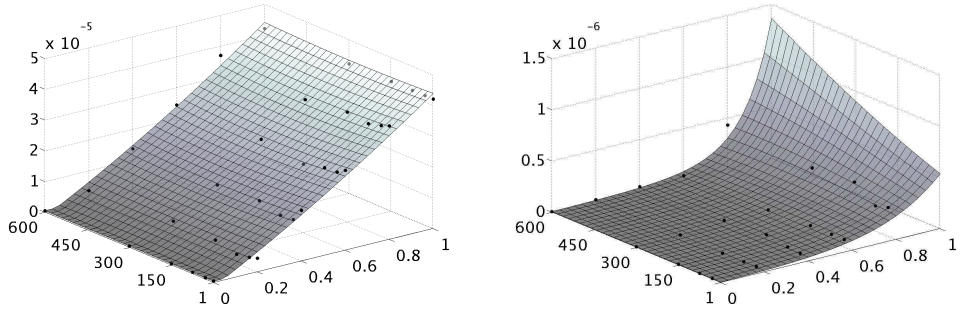

Figure 3: A visual comparison of $\mathscr{D}_w(\phi_w,\bar{x}), \mathscr{D}_i(\phi_w,\bar{x})$ with the entries of Tables 3 and 4 respectively. The control points are visualized with dots.

much faster rate than the chemical reaction and water have saturated the polymer across the entire thickness before significant scission takes place (Figure 4 top-left). Polymeric byproducts are produced almost homogeneously across the thickness of the coating and their consequent diffusion is responsible for conferring bulk erosion characteristics to the behavior of the reaction-diffusion system (Figure 4 bottom-left). Polymeric density $\tilde{\rho}$ decreases in a homogeneous fashion across the coating as smaller chains diffuse away (Figure 4 top and bottom-right). Such qualitative interpretation of polymer degradation can be profitably complemented with the analysis of the evolution of the system in the lumped state space $(\phi_w,\bar{x})$, reported in Figure 5. It shows that, because of fast water absorption and subsequent hydrolysis, the average degree of polymerization $\bar{x}$ quickly decreases and the water content of the mixture ϕ_w progressively increases. At the end of the process, most of the polymer in the mixture is in the range of small sub-fractions as confirmed by Figure 4 bottom-left.

Further information is obtained by analyzing how the mean value of the partial density of water and polymer, respectively defined as follows,

$$\bar{\rho}_w(t) = \frac{1}{L}\int_0^L \rho_w(t,z)dz, \quad \bar{\tilde{\rho}} = \frac{1}{L}\int_0^L \tilde{\rho}(t,z)dz$$

For a bulk eroding polymer such diagrams are expected to feature a sigmoid shape as confirmed by the results, reported in Figure 6.

Finally, we observe that the combination of microscale with macroscale models allows us to perform a quantitative validation, which is based on the comparison of the total density of the water/polymer mixture along the degradation process. On one hand, the microscale model provides, beside diffusivity, the total density of the mixture for different configurations of the system in the lumped state space, i.e. for different combinations of $(\phi_w,\bar{x})$. The results are reported in Table 2. On the other hand, the macroscale model is capable to represent how the mean value of total mixture density

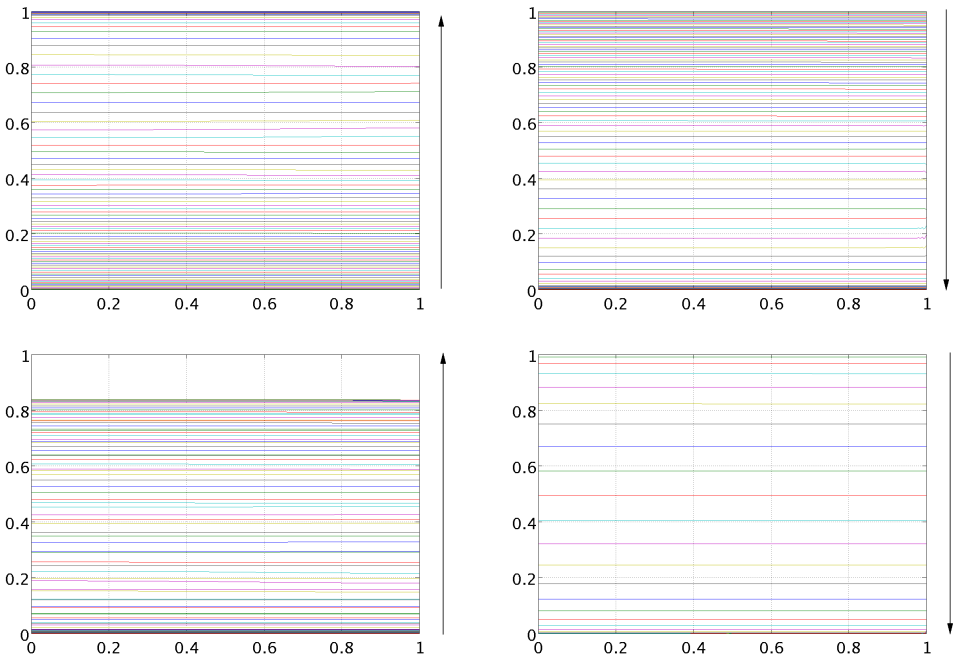

Figure 4: The non-dimensional partial densities $\rho_w(t,z)$, $\tilde{\rho}(t,z) = \sum_i \rho_i(t,z)$ are reported on top, while $\rho_1^{10} = \sum_{i=1}^{10} \rho_i(t,z)$, $\rho_{31}^{40} = \sum_{i=31}^{40} \rho_i(t,z)$ are depicted at the bottom. The abscissa represents the non-dimensional coordinate along the coating thickness, z, and the time evolution is indicated with the arrows on the right of each picture.

evolves in the lumped state space, that is

$$\bar{\rho}(\phi_w, \bar{x}) = \int_0^L \rho\big(\phi_w(t,z), \bar{x}(t,z)\big) dz$$

Such micro and macro-scale data are only indirectly correlated, because the macroscale model was fitted on the diffusivity provided by atomistic simulations. By consequence, their comparison represents a significant and quantitative indicator of the multiscale model capability to represent polymer degradation. In Figure 7, we represent on the left a biquadratic interpolation of the density dataset of Table 2 where the control points are depicted with dots. On this surface, we superpose the evolution of $\bar{\rho}(\phi_w, \bar{x})$ computed with the macroscale model. The agreement is rather satisfactory, as also confirmed by the transverse section at $\bar{x}_{300}$ of Figure 7 (left), which is reported on the right.

Acknowledgments

We acknowledge the Italian Institute of Technology with the Grant "Models and methods for degradable materials" and the European Research Council Advanced Grant

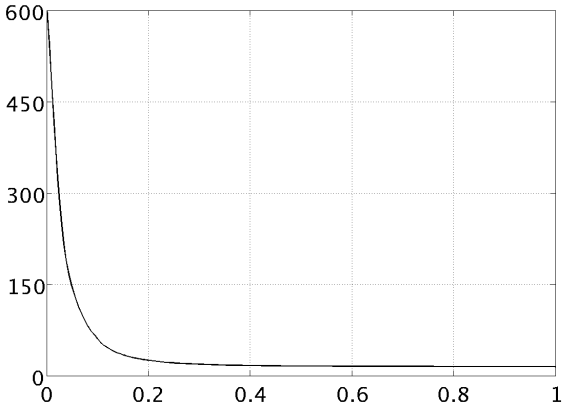

Figure 5: The trajectory of the system in the $(\phi_w, \bar{x})$ phase space.

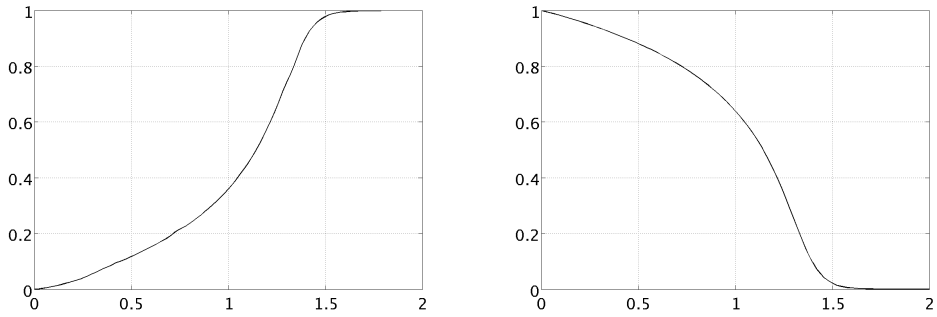

Figure 6: The mean value over $(0, L)$ of the non-dimensional partial density of water (left) and polymer (right).

"Mathcard, Mathematical Modelling and Simulation of the Cardiovascular System", Project ERC 2008 AdG 227058.

References

[1] C.M. Agrawal, R.B. Ray, Biodegradable polymeric scaffolds for musculoskeletal tissue engineering, J. Biomed. Mater. Res. 55 (2001) 141-150.

[2] S.A. Ali, P.J. Doherty, D.F. Williams, Mechanisms of polymer degradation in implantable devices. 2. Poly(dl-lactic acid), J. Biomed. Mater. Res. 27 (1993) 1409-1418.

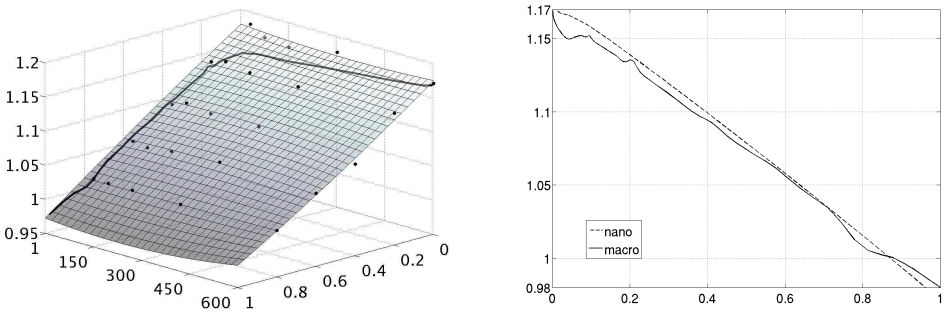

Figure 7: A comparison of the predicted water/polimer mixture densities provided by micro and macro-scale models (left). On the right we show a transverse section at $\bar{x}_{300}$.

[3] S.A. Ali, S.P. Zhong, P.J. Doherty, D.F. Williams, Mechanisms of polymer degradation in implantable devices. 1. Poly(caprolactone), Biomaterials 14 (1993) 648-656.

[4] M. Ballauff, B.A. Wolf, Degradation of chain molecules .1. Exact solution of the kinetic-equations, Macromolecules 14 (1981) 654-658.

[5] R.P. Batycky, J. Hanes, R. Langer, D.A. Edwards, A theoretical model of erosion and macromolecular drug release from biodegrading microspheres, J. Pharm. Sci. 86 (1997) 1464-1477.

[6] S.M. Bose, Y. Git, Mathematical modelling and computer simulation of linear polymer degradation: Simple scissions, Macromol. Theor. Simul. 13 (2004) 453-473.

[7] F.v. Burkersroda, L. Schedl, A. Gopferich, Why degradable polymers undergo surface erosion or bulk erosion, Biomaterials 23 (2002) 4221-4231.

[8] P. Deuflhard: A modified Newton method for the solution of ill-conditioned systems of nonlinear equations with application to multiple shooting, Numer. Math. 22 (1974), 289-315.

[9] A.M. Emsley, R.J. Heywood, Computer modeling of the degradation of linear-polymers, Polym. Degrad. Stabil. 49 (1995) 145-149.

[10] Entrialgo-Castano, M., A. Lendlein, et al. (2006). Molecular modeling investigations of dry and two water-swollen states of biodegradable polymers. Advanced Engineering Materials 8(5): 434-439.

[11] Gautieri, A., M. Ionita, et al. (2010). Computer-Aided Molecular Modeling and experimental validation of water permeability properties biosynthetic materials. Journal of Computational and Theoretical Nanoscience 7: 1-7.

[12] A. Gopferich, Polymer degradation and erosion: Mechanisms and applications, Eur. J. Pharm. Biopharm. 4 (1996) 1-11.

[13] A. Gopferich, Mechanisms of polymer degradation and elimination, in: A.J. Domb, J. Kost, D.M. Wiseman, (Eds), Handbook of biodegradable polymers, Drug targeting and delivery, Harwood Academic Publishers, Australia, 1997, pp. 451-471.

[14] A. Gopferich, R. Langer, Modeling polymer erosion, Macromolecules 26 (1993) 4105-4112.

[15] E. Hairer and G. Wanner: Solving ordinary differential equations II, Springer Series in Computational Mathematics 14, Springer-Verlag, Berlin, 2nd ed., 1996.

[16] T. Hayashi, Biodegradable polymers for biomedical uses, Prog. Polym. Sci. 19 (1994) 663-702.

[17] J. Heller, R.W. Baker, Theory and practice of controlled drug delivery from bioerodible polymers, in: R.W. Baker, (Ed), Controlled release of bioactive materials, Academic Press, New York, 1980, pp. 1-18.

[18] Hofmann, D., L. Fritz, et al. (2000). Detailed-atomistic molecular modeling of small molecule diffusion and solution processes in polymeric membrane materials. Macromolecular Theory and Simulations 9(6): 293-327.

[19] Ionita, M., D. Silvestri, et al. (2006). Diffusion of small molecules in bioartificial membranes for clinical use: molecular modelling and laboratory investigation. Desalination 200(1-3): 157-159.

[20] A. Joshi, K.J. Himmelstein, Dynamics of controlled release from bioerodible matrices, J. Control. Release 15 (1991) 95-104.

[21] A.M. Kotliar, S. Podgor, Evaluation of molecular size distributions and molecular weight averages resulting from random crosslinking and chain-scission processes, J. Polym. Sci. 55 (1961) 423-436.

[22] W. Kuhn, The kinetics of the decomposition of high molecular chains, Ber. Deut. Chem. Ges. 63 (1930) 1503-1509.

[23] R. Langer, Drug delivery and targeting, Nature 392 (1998) 5-10.

[24] H. Laufman, T. Rubel, Synthetic absorable sutures, Surg. Gynecol. Obstet. 145 (1977) 597-608.

[25] P.I. Lee, Diffusional release of a solute from a polymeric matrix – approximate analytical solutions, Journal of Membrane Science 7 (1980) 255-275.

[26] V. Lemaire, J. Belair, P. Hildgen, Structural modeling of drug release from biodegradable porous matrices based on a combined diffusion/erosion process, Int. J. Pharm. 258 (2003) 95-107.

[27] S.M. Li, S. McCarthy, Further investigations on the hydrolytic degradation of poly(dl-lactide), Biomaterials 20 (1999) 35-44.

[28] S. Li, H. Garreau, M. Vert, Structure-property relationships in the case of degradation of massive poly(-hydroxy acids) in aqueous media - part 3: Influence of the morphology of poly(l-lactic acid), Journal of Materials Science: Materials in Medicine S (1990) 198-206.

[29] S.M. Li, M. Vert, Morphological-changes resulting from the hydrolytic degradation of stereocopolymers derived from l-lactides and dl-lactides, Macromolecules 27 (1994) 3107-3110.

[30] R.A. Miller, J.M. Brady, D.E. Cutright, Degradation rates of oral resorbable implants (polylactates and polyglycolates): Rate modification with changes in pla/pga copolymer ratios, J. Biomed. Mater. Res. 11 (1977) 711-719.

[31] E.W. Montroll, R. Simha, Theory of depolymerization of long chain molecules, J. Chem. Phys. 8 (1940) 721-727.

[32] J. Moore, J. Soares, K. Rajagopal, Biodegradable stents: Biomechanical modeling challenges and opportunities, Cardiovascular Engineering and Technology 1 (2010) 52-65.

[33] T.Q. Nguyen, Kinetics of mechanochemical degradation by gel permeation chromatography, Polym. Degrad. Stabil. 46 (1994) 99-111.

[34] T.Q. Nguyen, H.H. Kausch, Gpc data interpretation in mechanochemical polymer degradation, Int. J. Polym. Anal. Ch. 4 (1998) 447-470.

[35] R.M. Ottenbrite, A.C. Albertsson, G. Scott, Discussion on degradation terminology, in: M. Vert, J. Feijen, A.C. Albertsson, G. Scott, E. Chiellini, (Eds), Biodegradable polymers and plastics, The Royal Society of Chemisty, Cambridge, 1992, pp. 73-92.

[36] S. Prabhu, S. Hossainy, Modeling of degradation and drug release from a biodegradable stent coating, J. Biomed. Mater. Res. A 80A (2007) 732-741.

[37] W.S. Pietrzak, D.R. Sarver, M.L. Verstynen, Bioabsorbable polymer science for the practicing surgeon, J. Craniofac. Surg. 8 (1997) 87-91.

[38] H. Pistner, D.R. Bendix, J. Muhling, J.F. Reuther, Poly(l-lactide) - a long-term degradation study in vivo .3. Analytical characterization, Biomaterials 14 (1993) 291-298.

[39] A. Quarteroni and A. Valli: Numerical approximation of partial differential equations, Springer Series in Computational Mathematics, 23, Springer-Verlag, Berlin, 1994.

[40] J. Siepmann, A. Gopferich, Mathematical modeling of bioerodible, polymeric drug delivery systems, Adv. Drug Deliver. Rev. 48 (2001) 229-247.

[41] Siparsky GL, Voorhees KJ, Dorgan JR, Schilling K. Water transport in polylactic acid (PLA), PLA/polycaprolactone copolymers, and PLA polyethylene glycol blends. Journal of Environmental Polymer Degradation. 5 (3):125-36, 1997.

[42] J.S. Soares, Bioabsorbable polymeric drug-eluting endovascular stents: A clinical review, Minerva Biotecnologica 21 (2009) 217-230.

[43] J.S. Soares, P. Zunino, A mixture model for water uptake, degradation, erosion, and drug release from polydisperse polymeric networks, Biomaterials 31 (2010) 3032-3042.

[44] Sun, H. (1998). COMPASS: An ab initio force-field optimized for condensed-phase applications - Overview with details on alkane and benzene compounds. Journal Of Physical Chemistry B 102(38): 7338-7364.

[45] J.A. Tamada, R. Langer, Erosion kinetics of hydrolytically degradable polymers, Proc. Natl. Acad. Sci. U. S. A. 90 (1993) 552-556.

[46] A.G. Thombre, Theoretical aspects of polymer biodegradation: Mathematical modeling of drug release and acid-catalyzed poly(otho-ester) biodegradation, in: M. Vert, J. Feijen, A.C. Albertsson, G. Scott, E. Chiellini, (Eds), Biodegradable polymers and plastics, The Royal Society of Chemisty, Cambridge, 1992, pp. 214-225.

[47] A.G. Thombre, K.J. Himmelstein, A simultaneous transport-reaction model for controlled drug delivery from catalyzed bioerodible polymer matrices, AIChE Journal 31 (1985) 759-766.

[48] M. Vert, S. Li, H. Garreau, J. Mauduit, M. Boustta, G. Schwach, R. Engel, J. Coudane, Complexity of the hydrolytic degradation of aliphatic polyesters, Angew. Markomol. Chemie 247 (1997) 239-253.

[49] X.S. Wu, N. Wang, Synthesis, characterization, biodegradation, and drug delivery application of biodegradable lactic/glycolic acid polymers. Part ii: Biodegradation, J. Biomater. Sci. Polym. Ed. 12 (2001) 21-34.

[50] K. Zygourakis, Development and temporal evolution of erosion fronts in bioerodible controlled release devices, Chemical Engineering Science 45 (1990) 2359-2366.

MOX Technical Reports, last issues

Dipartimento di Matematica "F. Brioschi",
Politecnico di Milano, Via Bonardi 9 - 20133 Milano (Italy)

10/2011 Zunino, P.; Vesentini, S.; Porpora, A.; Soares, J.S.; Gautieri, A.; Redaelli, A.
Multiscale computational analysis of degradable polymers

09/2011 Pigoli, D.; Sangalli, L.
Wavelets in Functional Data Analysis: estimation of multidimensional curves and their derivatives

08/2011 Ieva, F.; Paganoni, A.M.; Secchi, P.
Mining Administrative Health Databases for epidemiological purposes: a case study on Acute Myocardial Infarctions diagnoses

07/2011 Arioli, G.; Gamba, M.
Automatic computation of Chebyshev polynomials for the study of parameter dependence for hyperbolic systems

06/2011 Secchi, Piercesare; Stamm, Aymeric.; Vantini, Simone
Large p Small n Data: Inference for the Mean

05/2011 Arioli, Gianni; Gamba, Monica
An algorithm for the study of parameter dependence for hyperbolic systems

04/2011 Ieva, Francesca ; Paganoni, Anna Maria; Pigoli, Davide; Vitelli, Valeria
Multivariate functional clustering for the analysis of ECG curves morphology

03/2011 Garegnani, Giulia; Rosatti, Giorgio; Bonaventura, Luca
Mathematical and Numerical Modelling of Fully Coupled Mobile Bed Free Surface Flows

02/2011 Lassila, Toni; Quarteroni, Alfio; Rozza, Gianluigi
A reduced basis model with parametric coupling for fluid-structure interaction problems

01/2011 Dalla Rosa, M.; Sangalli, Laura M.; Vantini, Simone
Dimensional Reduction of Functional Data by means of Principal Differential Analysis